On the Take-Off of a Single-Wing Quadrotor

N A Aguillón, M Bonilla, S Salazar, Michel Malabre, V Azhmyakov

On the Take-Off of a Single-Wing Quadrotor

N.A. Aguillón*[1], M. Bonilla[2], S. Salazar[1], M. Malabre[3] and V. Azhmyakov[4]

***Abstract*— This paper focusses on differential thrust quadcopters, whose flight envelope can be divided in two, namely: the quadrotor flight envelope, and the airplane flight envelope. We define a transition maneuver as a controlled path followed by an aircraft in order to move between the two flight envelopes. We propose a control law that is robust with respect to wind disturbances and unmodeled aerodynamic effects. This approach ensures that the aircraft does not fall down during the transition maneuver.**

I. INTRODUCTION

Multicopters are the most popular type of small aircraft due to their ease-of-use. They have the ability of VTOL, but their payload capacity and endurance are both very compromised. The most popular type of multicopter is the quadcopter, with high reliability on a simple structural design [7]. In [8], two main types of Hybrid UAVs are distinguished, namely: convertiplanes and tail-sitters. The characteristic of tail-sitters is that they maintain their main body attitude vertical during take-off and landing maneuvers, but they have to change their body attitude for horizontal cruise flight [10], [11], [12]. For the tilt-rotor convertiplane case see for example [3].

This paper focusses on differential thrust multicopters, whose flight envelope can be divided in three, according to the magnitude of its angle of attack and its forward speed [5], namely: the hover flight envelope and the level flight envelope. Then a transition maneuver can be defined as the controlled path followed by an aircraft in order to move from the hover flight envelope to the level flight envelope or vice versa. The control law must be robust with respect to wind disturbances and unmodeled aerodynamic effects. And evenmore, the control law has to ensure that the aircraft does not fall down during the transition between the flight envelopes, Quadrotor Flight Envelope and Airplane Flight Envelope.

*The Ph.D. Student N.A. Aguillón is sponsered by CONACyT México

[1] N.A. Aguillón and S. Salazar are with CINVESTAV-IPN, Sistemas Autónomos de Navegación Aérea Y Submarina, UMI 3175 CINVESTAV-CNRS. A.P. 14-740. México 07000. nestor.aguillon@cinvestav.mx, sergio.salazar.cruz@gmail.com

[2] M. Bonilla is with the CINVESTAV-IPN, Control Automático, UMI 3575 CINVESTAV-CNRS, Mexico, e-mail: mbonilla@cinvestav.mx

[3] This work was done while Michel Malabre was with CNRS, LS2N, UMR 6004, Nantes, France. e-mail: michel.malabre@ls2n.fr

[4] Vadim Azhmyakov is with Facultad de Ingeniera y Ciencias Básicas, Universidad Central, Bogotá, Colombia, and with Institut für Theoretische Informatik, Mathematik und Operations Research, Universität der Bundeswehr München, München, Germany. vazhmyako@eafit.edu.co

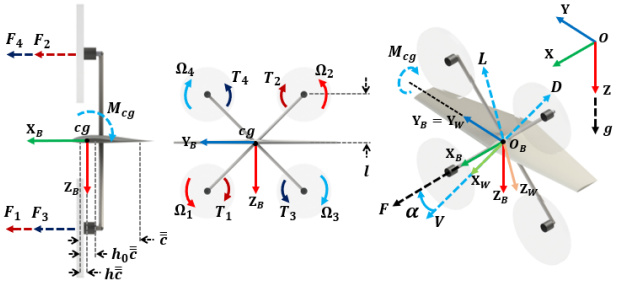

Fig. 1. Single-wing aircraft.

This paper deals with the control of the transition maneuver of a single-wing quadrotor Tail-Sitter. In §II we state the problem of changing from the Quadrotor Flight Envelope to the Aircraft Flight Envelope, ensuring that the aircraft does not fall down. In §III, we obtain an incremental state space representation. In §IV, we propose a control law which solves satisfactorily the stated problem in §II. In §V, we present simulation results. And finally, in §VI we conclude.

II. PROBLEM STATEMENT

Let us consider the *Single Wing Quadrotor Aircraft* (*SWQA*) shown in Fig. 1. The mechanical motion of the *SWQA* is considered in a fixed orthogonal axis set (earth axes) ($O\mathbf{XYZ}$), where $O\mathbf{Z}$ is a vertical axis, along the gravity vector $\begin{bmatrix} 0 & 0 & g \end{bmatrix}^T$. Let Φ, Θ and Ψ be the Euler angles, roll, pitch and yaw, measured with respect to the $O\mathbf{X}$, $O\mathbf{Y}$ and $O\mathbf{Z}$ axes, respectively[1]. Here ($O_B\mathbf{X}_B\mathbf{Y}_B\mathbf{Z}_B$) is the body axis system with its origin O_B fixed at the centre of gravity (c.g.) of the *SWQA* [4]. The total mass of the *SWQA* is equal to $m = 1.6$ [kg], and the moments of inertia with respect to the axis $O_B\mathbf{X}_B$, $O_B\mathbf{Y}_B$ and axis $O_B\mathbf{Z}_B$ are $I_x = 0.058$ [kg m^2], $I_y = 0.048$ [kg m^2] and $I_z = 0.052$ [kg m^2], respectively. We consider here the values, for the gravity: $g = 9.81$ [m s^{-2}], and for the air density: $\rho = 1.2$ [kg/m^3].

The single wing has a S5010 low speed airfoil for flying wings [9], with aspect ratio: $AR = 6$, span: $b = 1.35$ [m], mean aerodynamic chord: $\bar{\bar{c}} = 0.165$ [m], distance of the c.g. along $\bar{\bar{c}}$: $h = 0.1$, and location of the aerodynamic center: $h_0 \approx 0.25$. The aerodynamic coefficients at the quarter of $\bar{\bar{c}}$ are taken as (C_{L_0}, C_{L_1} [rad/^{o}]) = (0.1875, 0.0660), (C_{D_0}, C_{D_1} [rad/^{o}], C_{D_2} [rad^2/^{o}/^{o}]) = (0.0212, 0.0014, 0.0004), and (C_{M_0}, C_{M_1} [rad/^{o}]) = (-0.0134, 0.0092).

[1] Valid for $\Phi \approx \Psi \approx 0$. Here, the order of rotations from the earth axes to the body axes is $R_y R_x R_z$. This is an alternative definition which gives rise to the gimbal lock phenomenon at $\Phi = \pm\pi/2$ instead of at $\Theta = \pm\pi/2$.

We consider the problem of controlling the longitudinal motion of the SWQA (shown in Fig. 1), described by

$$\begin{bmatrix} d^2\mathbf{X}/dt^2 \\ d^2\mathbf{Z}/dt^2 \end{bmatrix} = -\frac{1}{m}\begin{bmatrix} \cos\Gamma & \sin\Gamma \\ -\sin\Gamma & \cos\Gamma \end{bmatrix}\begin{bmatrix} D(V,\alpha) \\ L(V,\alpha) \end{bmatrix} + \begin{bmatrix} 0 \\ g \end{bmatrix} + \frac{\mathcal{F}}{m}\begin{bmatrix} \cos\Theta \\ -\sin\Theta \end{bmatrix}, \tag{II.1}$$

$$\frac{d^2\Theta}{dt^2} = \frac{1}{I_y}(\mathcal{T}_q + M(V,\alpha) + \bar{\bar{c}}(h-h_0)L(V,\alpha)), \tag{II.2}$$

where $V = \sqrt{(d\mathbf{X}/dt)^2 + (d\mathbf{Z}/dt)^2}$ is the longitudinal flight speed, $\mathcal{F}$ is the total thrust of the rotors, $\mathcal{T}_q$ is the pitching moment, $L(V,\alpha) = q_\infty \mathcal{S}\big(\mathcal{C}_{\mathcal{L}_\alpha} + C_{L_1}\alpha\big)$, $D(V,\alpha) = q_\infty \mathcal{S}\big(\mathcal{C}_{\mathcal{D}_\alpha} + C_{D_1}\alpha + C_{D_2}\alpha^2\big)$ and $M(V,\alpha) = q_\infty \bar{\bar{c}}\,\mathcal{S}\big(\mathcal{C}_{\mathcal{M}_\alpha} + C_{M_1}\alpha\big)$ are the lift force, drag force, and pitching moment of the wing, respectively, $q_\infty = \rho V^2/2$ is the dynamic pressure, $\mathcal{S} = b^2/AR$ is the reference area, $\Gamma = \Theta - \alpha = \arctan\left(-(d\mathbf{Z}/dt)/(d\mathbf{X}/dt)\right)$ is called the flight path angle.

We distinguish two flight envelopes for the longitudinal dynamics, namely: the Quadrotor Flight Envelope (QFE) and the Airplane Flight Envelope (AFE); described as follows: 1) the QFE takes place when the total thrust of the rotors, $\mathcal{F}$, acts as the prime lift force, and arises at values of Θ around $\pi/2$, at low flight speed, V; and 2) the AFE takes place when the wing provides the prime lift force, $L(V,\alpha)$, and arises at large values of the flight speed, V, and small values of the angle of attack, α. Formally, we define these two flight envelopes in a similar way as in [5], as follows:

$$\begin{aligned} QFE &= \{(\alpha,V) : |\alpha| \leq 180[^o],\ V < 10[\text{m/s}]\}, \\ AFE &= \{(\alpha,V) : |\alpha| < 10[^o],\ V \geq 10[\text{m/s}]\}. \end{aligned} \tag{II.3}$$

We assume that, initially, the *SWQA* is with the rotors vertically oriented in hover flight, namely: $\Theta = 90^\circ$, in the QFE, with an initial flight speed of $V = 1$ [m/s]. Then we want the *SWQA* to move from the vertical flight state to a horizontal flight in the AFE, namely: we want to achieve a flight path angle of $\Gamma = 0^\circ$; a positive angle of attack, α, not bigger than 10°; and a final flight speed, V, of 15 [m/s]. The transition between these two flight envelopes must ensure that the *SWQA* will not fall down.

In order to solve this problem, we proceed as follows:

(i) We propose to track a take-off path, given in terms of the desired flight speed, $\overline{V}$, and the desired flight path angle, $\overline{\Gamma}$, the *SWQA* has to track a path such that:

$$d\overline{\mathbf{X}}/dt = \overline{V}\cos(\overline{\Gamma}), \quad d\overline{\mathbf{Z}}/dt = -\overline{V}\sin(\overline{\Gamma}), \tag{II.4}$$

where overlined variables, henceforth, denote the reference values of the respective variable. This allows us to write the variables of (II.1) and (II.2) as:

$$\begin{aligned} &\mathbf{X} = \overline{\mathbf{X}} + \mathbf{x};\quad \mathbf{Z} = \overline{\mathbf{Z}} + \mathbf{z};\quad V = \overline{V} + v;\quad \mathcal{F} = \overline{\mathcal{F}} + f; \\ &\Theta = \overline{\Theta} + \theta;\quad \Gamma = \overline{\Gamma} + \gamma;\quad \alpha = \overline{\alpha} + \alpha;\quad \mathcal{T}_q = \overline{\mathcal{T}}_q + \tau_q; \end{aligned} \tag{II.5}$$

where the lowercase variables, henceforth referred as incremental variables, stand for small increments around the reference values.

(ii) Given (II.4), we obtain the reference values of thrust, angle of attack, and pitching moment.

(iii) We translate our problem into the stabilization problem of the incremental variables. For this, in Section III we obtain a linear state space equation with piece-wise constant coefficients for the incremental variables.

(iv) In Section IV we propose an active disturbance rejection control law for the incremental dynamics.

From (II.4) and (II.1) we obtain

$$\begin{aligned} \begin{bmatrix} d^2\overline{\mathbf{X}}/dt^2 \\ d^2\overline{\mathbf{Z}}/dt^2 \end{bmatrix} &= \begin{bmatrix} \cos\overline{\Gamma}\,d\overline{V}/dt - \overline{V}\sin\overline{\Gamma}\,d\overline{\Gamma}/dt \\ -\sin\overline{\Gamma}\,d\overline{V}/dt - \overline{V}\cos\overline{\Gamma}\,d\overline{\Gamma}/dt \end{bmatrix} \\ &= \begin{bmatrix} 0 \\ g \end{bmatrix} - \frac{1}{m}\begin{bmatrix} \cos\overline{\Gamma} & \sin\overline{\Gamma} \\ -\sin\overline{\Gamma} & \cos\overline{\Gamma} \end{bmatrix}\begin{bmatrix} \overline{D} \\ \overline{L} \end{bmatrix} + \frac{\overline{\mathcal{F}}}{m}\begin{bmatrix} \cos\overline{\Theta} \\ -\sin\overline{\Theta} \end{bmatrix}. \end{aligned} \tag{II.6}$$

From (II.6), we deduce the trim values:

$$\begin{aligned} \begin{bmatrix} \overline{\mathcal{F}} \\ \overline{L} \end{bmatrix} = &\begin{bmatrix} \overline{D}/\cos\overline{\alpha} \\ -\overline{D}\tan\overline{\alpha} \end{bmatrix} + m\begin{bmatrix} g\sin\overline{\Gamma}/\cos\overline{\alpha} \\ g(\cos\overline{\Gamma} - \sin\overline{\Gamma}\tan\overline{\alpha}) \end{bmatrix} \\ &- m\begin{bmatrix} -d\overline{V}/dt/\cos\overline{\alpha} \\ \tan\overline{\alpha}\,d\overline{V}/dt - \overline{V}\,d\overline{\Gamma}/dt \end{bmatrix}, \end{aligned} \tag{II.7}$$

Assuming that $\overline{\alpha}$ remains small, we have that $\cos\overline{\alpha} \approx 1$ and $\sin\overline{\alpha} \approx \overline{\alpha}$, and, from $\overline{L}$ in (II.7), we get ($\bar{q}_\infty = \rho\overline{V}^2/2$):

$$\overline{\alpha} \approx \frac{mg\cos\overline{\Gamma} + m\overline{V}\frac{d\overline{\Gamma}}{dt} - \bar{q}_\infty \mathcal{S}\,C_{L_0}}{\bar{q}_\infty \mathcal{S}\,(C_{L_1} + C_{D_0}) + mg\sin\overline{\Gamma} + m\frac{d\overline{V}}{dt}}. \tag{II.8}$$

Given that $\Gamma = \Theta - \alpha$, and assuming that $\overline{\alpha}$ has a slow variation, we take $d\overline{\Theta}/dt := d\overline{\Gamma}/dt$, and from (II.2) we get

$$\frac{d^2\overline{\Theta}}{dt^2} = \frac{d^2\overline{\Gamma}}{dt^2} = \frac{1}{I_y}\left(\overline{\mathcal{T}}_q + \overline{M} + \bar{\bar{c}}(h-h_0)\overline{L}\right), \tag{II.9}$$

which gives the pitching moment trim value

$$\overline{\mathcal{T}}_q = I_y d^2\overline{\Gamma}/dt^2 - \overline{M} - \bar{\bar{c}}(h-h_0)\overline{L}. \tag{II.10}$$

III. STATE SPACE REPRESENTATION

a) $\mathbf{x}-\mathbf{z}$ *dynamic equations:* (II.1) and (II.6) imply:

$$\begin{aligned} \begin{bmatrix} d^2\mathbf{x}/dt^2 \\ d^2\mathbf{z}/dt^2 \end{bmatrix} = &\frac{\mathcal{F}}{m}\begin{bmatrix} \cos\Theta \\ -\sin\Theta \end{bmatrix} - \frac{\overline{\mathcal{F}}}{m}\begin{bmatrix} \cos\overline{\Theta} \\ -\sin\overline{\Theta} \end{bmatrix} \\ &- \frac{1}{m}\begin{bmatrix} \cos\Gamma & \sin\Gamma \\ -\sin\Gamma & \cos\Gamma \end{bmatrix}\begin{bmatrix} D \\ L \end{bmatrix} \\ &+ \begin{bmatrix} \cos\overline{\Gamma} & \sin\overline{\Gamma} \\ -\sin\overline{\Gamma} & \cos\overline{\Gamma} \end{bmatrix}\begin{bmatrix} \overline{D} \\ \overline{L} \end{bmatrix}, \end{aligned} \tag{III.1}$$

Expanding $L(V,\alpha)$ and $D(V,\alpha)$ in Taylor series, the lift and drag forces of the wing are expressed in incremental form as follows:

$$\begin{aligned} L(V,\alpha) &= \overline{L} + \mathring{L}_\alpha\alpha + \mathring{L}_v v + O(\alpha^2 + v^2), \\ D(V,\alpha) &= \overline{D} + \mathring{D}_\alpha\alpha + \mathring{D}_v v + O(\alpha^2 + v^2), \end{aligned} \tag{III.2}$$

where $\mathring{L}_\alpha = \bar{q}_\infty \mathcal{S}\,C_{L_2}$, $\mathring{L}_v = (\rho\overline{V})\mathcal{S}\,(C_{L_1} + C_{L_2}\overline{\alpha}_k)$, $\mathring{D}_\alpha = \bar{q}_\infty \mathcal{S}\,(C_{D_2} + 2C_{D_3}\overline{\alpha}_k)$, $\mathring{D}_v = (\rho\overline{V})\mathcal{S}\,(C_{D_1} + C_{D_2}\overline{\alpha}_k +$

$C_{D_3}\overline{\alpha}_k^2$). From (II.5), (III.1) and (III.2), we get

$$\begin{aligned}\begin{bmatrix} d^2\mathbf{x}/dt^2 \\ d^2\mathbf{z}/dt^2 \end{bmatrix} = &-\frac{1}{m}\begin{bmatrix} \cos\overline{\Gamma} & \sin\overline{\Gamma} \\ -\sin\overline{\Gamma} & \cos\overline{\Gamma} \end{bmatrix}\begin{bmatrix} 1 & \gamma \\ -\gamma & 1 \end{bmatrix}\begin{bmatrix} \overline{D} \\ \overline{L} \end{bmatrix} \\ &-\frac{1}{m}\begin{bmatrix} \cos\overline{\Gamma} & \sin\overline{\Gamma} \\ -\sin\overline{\Gamma} & \cos\overline{\Gamma} \end{bmatrix}\begin{bmatrix} \mathring{D}_\alpha & \mathring{D}_v \\ \mathring{L}_\alpha & \mathring{L}_v \end{bmatrix}\begin{bmatrix} \alpha \\ v \end{bmatrix} \\ &+\frac{1}{m}\begin{bmatrix} \cos\overline{\Theta} & -\overline{\mathcal{F}}\sin\overline{\Theta} \\ -\sin\overline{\Theta} & -\overline{\mathcal{F}}\cos\overline{\Theta} \end{bmatrix}\begin{bmatrix} f \\ \theta \end{bmatrix} + O(\delta_1)\end{aligned} \tag{III.3}$$

where $\delta_1 = \alpha^2 + \theta^2 + \gamma^2 + v^2 + f^2$.

Expanding V and Γ in Taylor series around their reference values, we obtain (recall (II.4), (II.5)):

$$\begin{aligned}\begin{bmatrix} v \\ \gamma \end{bmatrix} &= \begin{bmatrix} \cos\overline{\Gamma} & -\sin\overline{\Gamma} \\ -\sin\overline{\Gamma}/\overline{V} & -\cos\overline{\Gamma}/\overline{V} \end{bmatrix}\begin{bmatrix} d\mathbf{x}/dt \\ d\mathbf{z}/dt \end{bmatrix} + O(\delta_2) \\ \alpha &= \theta - \gamma.\end{aligned} \tag{III.4}$$

where $\delta_2 = (d\mathbf{x}/dt)^2 + (d\mathbf{z}/dt)^2$. Thus, from (III.4) and (III.3) we then get the incremental equations of $\mathbf{x}$ and $\mathbf{z}$:

$$\begin{aligned}\begin{bmatrix} d^2\mathbf{x}/dt^2 \\ d^2\mathbf{z}/dt^2 \end{bmatrix} = &\begin{bmatrix} \mathring{a}_{\mathbf{xx}} & \mathring{a}_{\mathbf{xz}} \\ \mathring{a}_{\mathbf{zx}} & \mathring{a}_{\mathbf{zz}} \end{bmatrix}\begin{bmatrix} d\mathbf{x}/dt \\ d\mathbf{z}/dt \end{bmatrix} + \begin{bmatrix} \mathring{a}_{\mathbf{x}f} & \mathring{a}_{\mathbf{x}\theta} \\ \mathring{a}_{\mathbf{z}f} & \mathring{a}_{\mathbf{z}\theta} \end{bmatrix}\begin{bmatrix} f \\ \theta \end{bmatrix} \\ &+ \mathfrak{q}_{_{ho}}\end{aligned} \tag{III.5}$$

where the coefficients $\mathring{a}_{ij}$, $i \in \{\mathbf{x}, \mathbf{z}\}$, $j \in \{\mathbf{x}, \mathbf{z}, \theta\}$, are functions of the reference values $\overline{V}$ and $\overline{\Gamma}$, and also of the coefficients $\mathring{L}_\alpha$, $\mathring{L}_v$, $\mathring{D}_\alpha$ and $\mathring{D}_v$. And $\mathfrak{q}_{_{ho}}$ is a disturbance term which takes into account the higher order terms of (III.3) and (III.4), namely: $\mathfrak{q}_{_{ho}} = O((d\mathbf{x}/dt)^2 + (d\mathbf{z}/dt)^2 + f^2 + \theta^2)$.

b) θ dynamic equation: From (II.2) and (II.9), we obtain the dynamic equation of the incremental pitch angle

$$\begin{aligned}d^2\theta/dt^2 = &\ (1/I_y)\left(\tau_q + M(V,\alpha) - \overline{M}\right. \\ &\left. -\bar{\bar{c}}(h-h_0)\left(L(V,\alpha) - \overline{L}\right)\right),\end{aligned} \tag{III.6}$$

The pitching moment of the wing, at the quarter of $\bar{\bar{c}}$, is expressed in incremental form as:

$$M(V,\alpha) = \overline{M} + \mathring{M}_\alpha\alpha + \mathring{M}_v v + O(\alpha^2 + v^2) \tag{III.7}$$

where

$$\begin{aligned}&\overline{M} = M(\overline{V},\overline{\alpha}), \quad \mathring{M}_\alpha = \tfrac{\partial M}{\partial\alpha}|_{\overline{V},\overline{\alpha}} = \bar{\bar{c}}\,\bar{q}_\infty\mathcal{S}\,C_{M_1} \\ &\mathring{M}_v = \tfrac{\partial M}{\partial V}|_{\overline{V},\overline{\alpha}} = \bar{\bar{c}}\,(\rho\overline{V})\mathcal{S}\,C_M(\overline{\alpha})\end{aligned} \tag{III.8}$$

Thus, from (III.2), (III.4) and (III.7), we get the incremental equations of the θ dynamics

$$\frac{d^2\theta}{dt^2} = \frac{1}{I_y}\tau_q + \mathring{a}_{\theta\mathbf{x}}\frac{d\mathbf{x}}{dt} + \mathring{a}_{\theta\mathbf{z}}\frac{d\mathbf{z}}{dt} + \mathring{a}_{\theta\theta}\theta + \mathfrak{q}_\theta, \tag{III.9}$$

where the coefficients $\mathring{a}_{\theta j}$, $j \in \{\mathbf{x}, \mathbf{z}, \theta\}$, are functions of the reference values $\overline{V}$ and $\overline{\Gamma}$, and also of the coefficients (III.8). And $\mathfrak{q}_\theta$ is a disturbance term from the higher order terms in (III.7), namely (recall (III.4)): $\mathfrak{q}_\theta = O\left((d\mathbf{x}/dt)^2 + (d\mathbf{z}/dt)^2\right)$.

c) Piece-wise constant incremental equations with constant input coefficients: Let us note that (III.5) has the inconvenient that the input variable f is acting through variable coefficients $\mathring{a}_{\mathbf{x}f}$ and $\mathring{a}_{\mathbf{z}f}$. To overcome this inconvenient we propose the following piece-wise constant coordinate transformation.

$$\begin{bmatrix} \hat{\mathbf{X}} \\ \hat{\mathbf{Z}} \end{bmatrix} = \begin{bmatrix} \cos\overline{\Theta}_k & -\sin\overline{\Theta}_k \\ \sin\overline{\Theta}_k & \cos\overline{\Theta}_k \end{bmatrix}\begin{bmatrix} \mathbf{X} \\ \mathbf{Z} \end{bmatrix} \tag{III.10}$$

where $\overline{\Theta}_k(t) = \overline{\Theta}(t_k)\ \forall t \in (t_k, t_{k+1}]$, $k \in \{0, \ldots, N-1\}$, according to the partition of the transition time interval:

$$\{(t_0, t_1], (t_1, t_2], \ldots, (t_{N-1}, t_N]\}.$$

From (III.10), we obtain the $\hat{\mathbf{x}} - \hat{\mathbf{z}}$ incremental dynamic equations:

$$\begin{aligned}\begin{bmatrix} d^2\hat{\mathbf{x}}/dt^2 \\ d^2\hat{\mathbf{z}}/dt^2 \end{bmatrix} = &\begin{bmatrix} \mathring{a}_{22k} & \mathring{a}_{24k} \\ \mathring{a}_{42k} & \mathring{a}_{44k} \end{bmatrix}\begin{bmatrix} d\hat{\mathbf{x}}/dt \\ d\hat{\mathbf{z}}/dt \end{bmatrix} \\ &+ \begin{bmatrix} 1/m & \mathring{a}_{25k} \\ 0 & \mathring{a}_{45k} \end{bmatrix}\begin{bmatrix} f \\ \theta \end{bmatrix} + \begin{bmatrix} \mathfrak{q}_{\mathbf{x}k} \\ \mathfrak{q}_{\mathbf{z}k} \end{bmatrix}, \\ \frac{d^2\theta}{dt^2} = &\ \frac{1}{I_y}\tau_q + \mathring{a}_{62k}\frac{d\hat{\mathbf{x}}}{dt} + \mathring{a}_{64k}\frac{d\hat{\mathbf{z}}}{dt} + \mathring{a}_{65k}\theta + \mathfrak{q}_{\theta k},\end{aligned} \tag{III.11}$$

where the coefficients $\mathring{a}_{ijk}$, $i \in \{2, 4, 6\}$, $j \in \{2, 4, 5\}$, are given in detail in Appendix A. They are defined by

$$\mathring{a}_{ij}(t) = \mathring{a}_{ijk} + \delta_{ij}(t), \quad t \in (t_k, t_{k+1}],\ k \in \{0, \ldots, N-1\}, \tag{III.12}$$

where $\mathring{a}_{ijk} = \mathring{a}_{ij}(t_k)$; and the variables $\mathfrak{q}_{_{jk}}(t)$, $j \in \{\mathbf{x}, \mathbf{z}, \theta\}$, take into account the incremental time varying terms $\delta_{ij}(t)$.

Let us note that the input variable f in (III.11) is now acting through piece-wise constant coefficients.

d) Piece-wise constant state space representation: From (III.11), we obtain the state space representation of the incremental longitudinal dynamics of the *SWQA* ($\Sigma_k(A_{qk}, B, S, C)$, $k \in \{1, \ldots, N\}$):

$$dx/dt = A_{q_k}x + Bu + S\mathfrak{q}\,, \quad y = Cx, \tag{III.13}$$

where $x = \begin{bmatrix} x_{\mathbf{x}} & x_{\mathbf{z}} & x_\theta \end{bmatrix}^T$, $x_{\mathbf{x}} = \begin{bmatrix} \hat{\mathbf{x}} & d\hat{\mathbf{x}}/dt \end{bmatrix}^T$, $x_{\mathbf{z}} = \begin{bmatrix} \hat{\mathbf{z}} & d\hat{\mathbf{z}}/dt \end{bmatrix}^T$, $x_\theta = \begin{bmatrix} \theta & d\theta/dt \end{bmatrix}^T$, $u = \begin{bmatrix} f & \tau_q \end{bmatrix}^T$, $\mathfrak{q} = \begin{bmatrix} \mathfrak{q}_{\mathbf{x}k} & \mathfrak{q}_{\mathbf{z}k} & \mathfrak{q}_{\theta k} \end{bmatrix}^T$, $y = \begin{bmatrix} \hat{\mathbf{x}} & \hat{\mathbf{z}} \end{bmatrix}^T$, and

$$A_{q_k} = \left[\begin{array}{cc|cc|cc} 0 & 1 & 0 & 0 & 0 & 0 \\ 0 & \mathring{a}_{22k} & 0 & \mathring{a}_{24k} & \mathring{a}_{25k} & 0 \\ \hline 0 & 0 & 0 & 1 & 0 & 0 \\ 0 & \mathring{a}_{42k} & 0 & \mathring{a}_{44k} & \mathring{a}_{45k} & 0 \\ \hline 0 & 0 & 0 & 0 & 0 & 1 \\ 0 & \mathring{a}_{62k} & 0 & \mathring{a}_{64k} & \mathring{a}_{65k} & 0 \end{array}\right],$$

$$B = \left[\begin{array}{cc} 0 & 0 \\ 1/m & 0 \\ \hline 0 & 0 \\ 0 & 0 \\ \hline 0 & 0 \\ 0 & 1/I_y \end{array}\right],\ S = \left[\begin{array}{ccc} 0 & 0 & 0 \\ 1 & 0 & 0 \\ \hline 0 & 0 & 0 \\ 0 & 1 & 0 \\ \hline 0 & 0 & 0 \\ 0 & 0 & 1 \end{array}\right],\ C = \left[\begin{array}{cc} 1 & 0 \\ 0 & 0 \\ \hline 0 & 1 \\ 0 & 0 \\ \hline 0 & 0 \\ 0 & 0 \end{array}\right]^T. \tag{III.14}$$

IV. CONTROL LAW

In Section II we have stated the problem of controlling the longitudinal motion of the SWQA, in order to achieve the transition from the QFE to the AFE. For this, we have to track the proposed path, defined by (II.4), ensuring a positive angle of attack, $\alpha \leq 10$ [^{o}], and a final flight speed $V(t_N) = 15$ [m/s].

In Section III we have obtained the state-space representation (III.13), which describes the behavior of the incremental variables, $\mathbf{x}$, $\mathbf{z}$, θ, around the reference values defined by $\overline{V}$ and $\overline{\Gamma}$. In this state space representation, $\mathfrak{q}$ is a disturbance term which takes into account the nonlinear (higher order) terms which tend to zero when the SWQA dynamics tends to the reference trajectory given by $\overline{V}$ and $\overline{\Gamma}$.

Thus, the control law has to ensure the stability of the non-disturbed state space representations ($q = 0$): $\Sigma_k(A_{qk}, B, C)$, $k \in \{1, \ldots, N\}$ (*cf.* (III.13)), and also the compensation of the disturbance term, q, in the stabilized state space representation (III.13), namely:

$$u = \overline{u} + \hat{u} \tag{IV.1}$$

where $\overline{u} = Fx$ is a reference linear stabilizing state feedback [2], [6]; and $\hat{u}$ is a disturbance rejection term, based on the Beard-Jones filter [1], which compensates the effects of $\overline{q}$ on the output. These two terms are described hereafter.

A. Nominal linear feedback term

The inner control law, $\overline{u} = Fx$, stabilizes the N state space representations, $\Sigma(A_{qk}, B, C)$. For this, we proceed as follows [2]:

1) We first choose a convenient value $j \in \{1, \ldots, N\}$ for k in (III.14), and we define the reference state matrix

$$\overline{A} = \overline{A}_{q_j}. \tag{IV.2}$$

2) We next solve the Ricatti equation

$$\overline{A}^T P_0 + P_0 \overline{A} - P_0 B \overline{R}^{-1} B^T P_0 = -\overline{Q}_0. \tag{IV.3}$$

for P_0, where $\overline{Q}_0$ and $\overline{R}$ are symmetric positive definite matrices.

3) We then check that the stability conditions [2]

$$\lambda_{min}\left((\overline{A} - A_{qk})^T P_0 + P_0(\overline{A} - A_{qk})\right) + \lambda_{min}(\overline{Q}_0) > 0. \tag{IV.4}$$

hold for all $k \in \{1, \ldots, N\}$. If it is not the case, then choose a new $\overline{Q}_0$ and $\overline{R}$, and go again to item 2).

4) We finally define the state feedback:

$$\bar{u} = -Fx\,, \quad F = \overline{R}^{-1} B^T P_0\,. \tag{IV.5}$$

[2]see Appendix B

B. Disturbance rejection term

From (III.13), (IV.1) and (IV.5), we get

$$dx/dt = A_{\scriptscriptstyle F} x + B\hat{u} + S\overline{\mathfrak{q}}\,, \quad y = Cx \tag{IV.6}$$

where $A_{\scriptscriptstyle F} = \overline{A} - BF$, and $S\overline{\mathfrak{q}} = S\mathfrak{q} + (A_{qk} - \overline{A})x$.

In [1], we have shown that $\overline{\mathfrak{q}}$ can be estimated with the Beard-Jones Filter:

$$d\hat{x}/dt = A_{\scriptscriptstyle K}\hat{x} - K_o y + B\hat{u}\,, \quad \hat{u} = H^{\ell}(C\hat{x} - y)\,, \tag{IV.7}$$

where $A_{\scriptscriptstyle K} = A_{\scriptscriptstyle F} + K_o C$, $K_o \in \mathbb{R}^{6\times 2}$ is an output injection gain such that $A_{\scriptscriptstyle K}$ is Hurwitz, $H = -CA_{\scriptscriptstyle K}^{-1}B$, and H^{ℓ} denotes a left inverse of H. Let us take

$$K_o = T\left(\overline{K} - \widehat{K}\right), \tag{IV.8}$$

where T and $\overline{K}$ are given in Appendix C, and

$$\widehat{K} = \begin{bmatrix} k_{12} & k_{11} & 0 & 0 & 0 & 0 \\ 0 & 0 & k_{24} & k_{23} & k_{22} & k_{21} \end{bmatrix}^T. \tag{IV.9}$$

V. SIMULATION RESULTS

The proposed methodology is implemented in two simulation scenarios. In the first scenario, the incremental dynamic (III.5)-(III.9) is stabilized using only the state feedback term in (IV.1). In the second scenario, we applied both the stabilizing control law (IV.5) and the Beard-Jones filter (IV.7), and we considered an external disturbance term, d, introduced to the translational equation (II.1).

Let us first define the desired transition path in terms of the reference speed and flight path angle:

$$\begin{aligned} \overline{V} &= \overline{V}_0 + \left(\overline{V}_N - \overline{V}_0\right)\left(1 - \cos\left(\pi t/t_N\right)\right)/2 \\ d\overline{V}/dt &= \pi\left(\overline{V}_N - \overline{V}_0\right)\,\sin\left(\pi t/t_N\right)/\left(2t_N\right) \\ \overline{\Gamma} &= (\pi/2) - (\pi/4)\left(1 - \cos\left(\pi t/t_N\right)\right) \\ d\overline{\Gamma}/dt &= -\pi^2 \sin\left(\pi t/t_N\right)/\left(4t_N\right) \\ d^2\overline{\Gamma}/dt^2 &= -\pi^3 \cos\left(\pi t/t_N\right)/\left(4t_N^2\right) \end{aligned} \tag{V.1}$$

where $t_N = 5$ [s] is the transition time, and $\overline{V}_0 = 1$ [m/s] and $\overline{V}_N = 15$ [m/s] are the initial speed and the final flight speed, respectively. The transition time interval is partitioned in $N = 10$ sub intervals, where $t_k = (k/N)^{475/1918}$, $k = 0, \ldots, N$. Notice that this choice of the take-off path gives $d\overline{V}/dt(t_k) = 0$ and $d\overline{\Gamma}/dt(t_k) = 0$ when $t_k \in \{0, N\}$, which reduces the values of $\overline{\alpha}$ and $\overline{\mathcal{F}}$ at the path boundaries.

With respect to $\overline{A}$ in (IV.2), we set $j = 10$, namely (see (III.14) and Appendix A):

$$\overline{A} = \begin{bmatrix} 0 & 1 & 0 & 0 & 0 & 0 \\ 0 & -0.062 & 0 & 0.619 & -0.4863 & 0 \\ 0 & 0 & 0 & 1 & 0 & 0 \\ 0 & -0.9689 & 0 & -6.4664 & -96.614 & 0 \\ 0 & 0 & 0 & 0 & 0 & 1 \\ 0 & -0.5151 & 0 & -5.621 & -5.5862 & 0 \end{bmatrix}. \tag{V.2}$$

TABLE I

STABILITY CONDITION (IV.4): $\lambda_k^* = \lambda_{min}(\overline{Q}_0) + \lambda_{min}\Big((\overline{A} - A_{q_k})^T P_0 + P_0(\overline{A} - A_{q_k})\Big)$, $\lambda_{min}(\overline{Q}_0) = 1$.

k	1	2	3	4	5
λ_k^*	0.01	0.34	0.55	0.68	0.76
k	6	7	8	9	10
λ_k^*	0.82	0.86	0.87	0.78	1

A. First simulation scenario: state feedback

In this scenario, we only considered the reference stabilizing term (IV.5) in (IV.1) and (IV.3), where

$$Q_0 = \left[Q_{i,j}\right], \quad Q_{i,j} = \begin{cases} 1, & i \in \{1, \ldots, 4\},\ j = i, \\ 2, & i \in \{5,\ 6\},\ j = i, \\ 0, & j \neq i, \end{cases}$$
$$R = \begin{bmatrix} 1/20 & 0 \\ 0 & 1 \end{bmatrix}, \tag{V.3}$$

which gave the state feedback

$$F = \begin{bmatrix} 4.4318 & 5.6952 & -0.5995 & 0.1878 \\ -0.134 & -0.073 & -0.991 & -0.6647 \\ -1.5491 & -0.0438 \\ 12.748 & 1.7955 \end{bmatrix}, \tag{V.4}$$

and the closed loop eigenvalues

$$\sigma(\overline{A} + BF) = \{ -29.214, -2.6677, -0.9599, \\ -1.0586, -6.7967 \pm 4.9845j\}, \tag{V.5}$$

where the complex conjugate pair of eigenvalues in (V.5) has a damping coefficient of 0.806. The stability condition (IV.4) is satisfied for all k in (III.14), as shown in Table I.

B. Second scenario: Disturbance compensation

In this scenario, we add the disturbance term

$$d = \begin{bmatrix} 1.5 & 0.5 \end{bmatrix}^T \sin\left(1.1\pi \sin\left(\pi t / t_N\right) + 1\right) \tag{V.6}$$

to the right side of (II.1). The effect of this disturbance signal is compensated at the output, y, by the Beard-Jones filter.

For the syntesis of the Beard-Jones filter, we follows Example 3 of [1]. For this, we propose $\overline{\pi}_{wx}(s) = (s + a_x)$ and $\pi_{ex}(s) = s\overline{\pi}_{wx}(s) + b_x = (s + \rho_x)^2$, where $a_x = 2\rho_x$, $b_x = \rho_x^2$. And $\overline{\pi}_{wz}(s) = (s + a_z)(s^2 + a_z s + b_z)$ and $\pi_{ez}(s) = s\overline{\pi}_{wz}(s) + c_z = (s+\rho_z)^2(s + r\rho_z)^2$, where $a_z = (r+1)\rho_z$, $b_z = 2r\rho_z^2$, $c_z = r^2\rho_z^4$, and where the damping coefficient of the second degree polynomial of $\overline{\pi}_{wz}(s)$ is $\zeta = (r+1)/\sqrt{8r}$.

Based on Corollary 1 of [1], the scalar r is chosen as $r = 6$, resulting in the damping coefficient $\zeta = 1.01$; and $\rho_x = 4.25$ and $\rho_z = 5.51$, resulting in the cut frequencies: $\omega_{c_x} = \omega_{c_z} = 3$ [rad/s], which are more than five times greater than the smallest eigenvalue of (V.2), given in (V.5), and at least two times the largest frequency component of d. The resulting Beard-Jones filter coefficients for the $x_{\mathbf{x}}$ subsystem are: $k_{11} = 8.5$ and $k_{12} = 18.06$; and for the $x_{\mathbf{z}} - x_\theta$ subsystem: $k_{21} = 77.14$, $k_{22} = 1852$, $k_{23} = 14052$, $k_{24} = 33182$.

In order to evaluate the results, let us introduce the Integral of the Absolute value of the Error (IAE), defined by

$$IAE = \frac{1}{t_N}\int_0^{t_N} |e|\, dt. \tag{V.7}$$

The IAE (V.7) gives the mean value of the error along the take-off path on both simulation scenarios, as summarized in Table II.

TABLE II

IAE	$e = y = [\hat{\mathbf{x}}\ \ \hat{\mathbf{z}}]^T$	$e = d\mathbf{y}/dt = [d\hat{\mathbf{x}}/dt\ \ \ d\hat{\mathbf{z}}/dt]^T$
Scenario1	0.03144	0.0432
Scenario 2	0.2762	0.5699

VI. CONCLUDING REMARKS

In Fig. 2 we show the tracking of the absolute position, absolute velocity, and pitch angle, as well as the evolution of the output, for the two simulation scenarios. From Table II, the deviation from the reference absolute position (velocity) remains less than a few centimeters (per second) on both simulation scenarios. This means that the transition maneuver performed as expected.

In Fig. 3 we show the evolution of the input signals. From Fig. 3(a) we can note that the airplane does not fall down, as the weight of the aircraft is always compensated by the thrust and the lift during the entire flight. The incremental thrust component remained small enough to maintain the total thrust under 40% above the *SWQA* weight. In Fig. 3(b), we show some spikes from the discontinuous nature of the change of variable (III.10), which have no significant effects on the tracking performance shown in Fig. 2. From Fig. 3C we verify that the angle of attack remains small enough over the transition between flight envelopes (QFE and AFE) [3].

REFERENCES

[1] Bonilla, M., L.A. Blas, V. Azhmyakov, M. Malabre, S. Salazar. Robust structural feedback linearization based on the nonlinearities rejection. *Journal of the Franklin Institute*, vol. 357(4), pp. 2232 – 2262, 2020.

[2] Bonilla, M., N.A. Aguillon, M A Ortiz, J.J. Loiseau, M Malabre, V. Azhmyakov, S. Salazar. Stabilization of a class of switched dynamic systems: The Ricatti equation based approach. 2020, *Submitted to IMA Journal of Mathematical Control and Informaiton*.

[3] Cardoso, D.N., S. Esteban, G.V. Raffo. A new robust adaptive mixing control for trajectory tracking with improved forward flight of a tilt-rotor UAV. *ISA Transactions*, 19 pp., 2020.

[4] Cook, M. **Flight Dynamics Principles. A Linear Systems Approach to Aircraft Stability and Control**, 3rd ed. *Elsevier*, 2013.

[5] Naldi, R., L. Marconi. Optimal transition maneuvers for a class of V/STOL aircraft, *Automatica*, vol. 47, no. 5, pp. 870 – 879, 2011.

[6] Ortiz, M., M. Bonilla, J.J. Loiseau, M. Malabre, V. Azhmyakov. On the LQ based stabilization for a class of switched dynamic systems. *1st Virtual IFAC World Congress (IFAC-V 2020)*, 2020.

[7] Quan, Q. **Introduction to multicopter design and control**. *Springer* 2017.

[8] Saeed, A.S., A.B. Younes, S. Islam, J. Dias, L. Seneviratne, G. Cai. A review on the platform design, dynamic modeling and control of hybrid UAVs. *2015 International Conference on Unmanned Aircraft Systems (ICUAS)*, 2015, pp. 806–815.

[3] At the first instants, in the initial hover condition, the angle of attack actually gets under -20^o, but it immediately gets inside the desired gap, $|\alpha| < 10^o$.

[9] Selig, M., C. Lyon, P. Gigure, C. Ninham , J. Guglielmo. **Summary of Low-Speed Airfoil Data**. *SoarTech Publications*, 1996, vol. 2.

[10] Sinha, P., P. Esden-Tempski, C.A. Forrette, J.K. Gibboney, G.M. Horn,. Versatile, modular, extensible vtol aerial platform with autonomous flight mode transitions. *2012 IEEE Aerospace Conference*, 2012, pp. 1–17.

[11] Theys, B., G. De Vos, J. De Schutter. A control approach for transitioning VTOL UAVs with continuously varying transition angle and controlled by differential thrust. *2016 International Conference on Unmanned Aircraft Systems (ICUAS)*, 2016, pp. 118–125.

[12] Vorsin, D., S. Arogeti. Flight transition control of a multipurpose UAV. *2017 13th IEEE International Conference on Control Automation (ICCA)*, 2017, pp. 507–512.

APPENDIX

A. Coefficients of (III.11)

$$
\begin{aligned}
\mathring{a}_{22k} &\approx \left(m\,\overline{V}_k\right)^{-1}\Big(-\mathring{D}_{vk}\,\overline{V}_k+\left(\mathring{D}_{\alpha k}-\overline{L}_k+\mathring{L}_{vk}\,\overline{V}_k\right)\overline{\alpha}_k\Big),\\
\mathring{a}_{24k} &\approx \left(m\,\overline{V}_k\right)^{-1}\Big(\overline{L}_k-\mathring{D}_{\alpha k}+\left(\overline{D}_k+\mathring{L}_{\alpha k}-\mathring{D}_{vk}\,\overline{V}_k\right)\overline{\alpha}_k\Big),\\
\mathring{a}_{25k} &\approx m^{-1}\left(-\mathring{D}_{\alpha k}+\mathring{L}_{\alpha k}\,\overline{\alpha}_k\right),\\
\mathring{a}_{42k} &\approx \frac{m}{\overline{V}_k}\Big(\mathring{D}_{\alpha k}-\mathring{L}_{vk}\,\overline{V}_k+\left(\overline{D}_k+\mathring{L}_{\alpha k}-\mathring{D}_{vk}\,\overline{V}_k\right)\overline{\alpha}_k\Big),\\
\mathring{a}_{44k} &\approx \frac{m}{\overline{V}_k}\Big(-\overline{D}_k-\mathring{L}_{\alpha k}+2\left(\mathring{D}_{\alpha k}-\overline{L}_k+\mathring{L}_{vk}\,\overline{V}_k\right)\overline{\alpha}_k\Big),\\
\mathring{a}_{45k} &\approx -m^{-1}\left(\overline{\mathcal{F}}_k+\mathring{L}_{\alpha k}+\mathring{D}_{\alpha k}\,\overline{\alpha}_k\right),\\
\mathring{a}_{62k} &\approx I_y^{-1}\left(\mathring{M}_{vk}+\bar{\bar{c}}(h-h_0)\,\mathring{L}_{vk}\right)-\mathring{a}_{65k}\,\overline{\alpha}_k,\\
\mathring{a}_{64k} &\approx \mathring{a}_{65k}+I_y^{-1}\left(\mathring{M}_{vk}+\bar{\bar{c}}(h-h_0)\,\mathring{L}_{vk}\right)\overline{\alpha}_k,\\
\mathring{a}_{65k} &= I_y^{-1}\left(\mathring{M}_{\alpha k}+\bar{\bar{c}}(h-h_0)\,\mathring{L}_{\alpha k}\right)
\end{aligned}
$$

where $\overline{L}_k=\overline{L}(t_k)$, $\overline{D}_k=\overline{D}(t_k)$, $\overline{M}_k=\overline{M}(t_k)$, $\mathring{L}_{vk}=\mathring{L}_v(t_k)$, $\mathring{D}_{vk}=\mathring{D}_v(t_k)$, $\mathring{M}_{vk}=\mathring{M}_v(t_k)$, $\mathring{L}_{\alpha k}=\mathring{L}_\alpha(t_k)$, $\mathring{D}_{\alpha k}=\mathring{D}_\alpha(t_k)$, $\mathring{M}_{\alpha k}=\mathring{M}_\alpha(t_k)$, $\overline{\alpha}_k=\overline{\alpha}(t_k)$, $\overline{V}_k=\overline{V}(t_k)$, $\overline{\mathcal{F}}_k=\overline{\mathcal{F}}(t_k)$.

B. Sketch of the proof of the stability condition

Applying the inner control law (IV.5) to the undisturbed state space representation, (III.13), we get the inner closed loop system

$$\frac{dx}{dt}=\left(A_{qk}-B\overline{R}^{-1}B^TP_0\right)x \tag{B.1}$$

Let us define the Lyapunov function candidate

$$\mathcal{V}(x)=x^TP_0x \tag{B.2}$$

where $P_0>0$ is the solution of (IV.3). Deriving the Lyapunov function candidate (B.2) along the trajectories of the inner closed loop system (B.1), we have (recall (IV.3) and (IV.5))

$$
\begin{aligned}
\tfrac{d}{dt}\mathcal{V} &= x^T\Big(P_0\left(A_{qk}-B\overline{R}^{-1}B^TP_0\right)\\
&\qquad+\left(A_{qk}^T-P_0B\overline{R}^{-1}B^T\right)P_0\Big)x\\
&= -x^T\left(\overline{Q}_0+F^T\overline{R}F+\left(\overline{A}-A_{qk}\right)^TP_0+P_0\left(\overline{A}-A_{qk}\right)\right)x
\end{aligned}
\tag{B.3}
$$

Notice in (B.3) that $F^T\overline{R}F\geq 0$. Then, a sufficient condition to ensure that (B.3) is a negative definite function is

$$\lambda_{\min}\left(\overline{Q}_0\right)+\lambda_{\min}\left(\left(\overline{A}-A_{qk}\right)^TP_0+P_0\left(\overline{A}-A_{qk}\right)\right)>0 \tag{B.4}$$

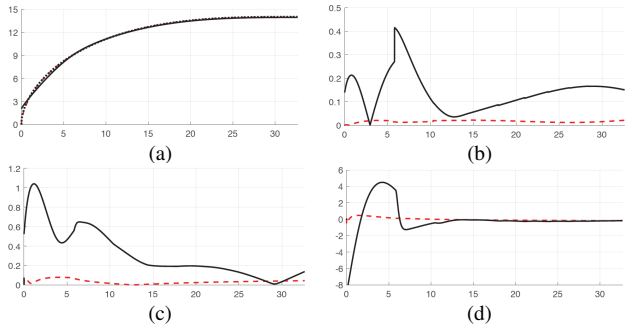

Fig. 2. Simulation results for the first scenario (dashed red lines), second scenario (dash-dotted blue lines), and third scenario (solid black lines). a) Resulting position on the vertical plane: $-\overline{\mathbf{Z}}$ *v.s.* $\overline{\mathbf{X}}$, b) norm of the output $y=[\hat{\mathbf{x}}\ \ \hat{\mathbf{z}}]^T$: $\|y\|$ *v.s.* $\overline{\mathbf{X}}$, c) norm of the time derivative of the output: $\|dy/dt\|$ *v.s.* $\overline{\mathbf{X}}$, and d) incremental pitch angle: θ *v.s.* $\overline{\mathbf{X}}$.

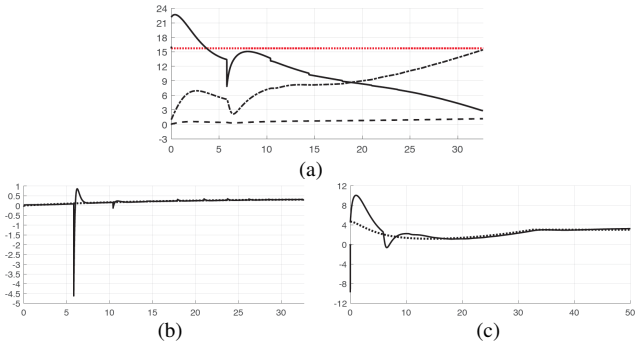

Fig. 3. Forces acting on the body and angle of attack of the third scenario. a) weight (dotted red line), thrust (solid black line), lift of the wing (dash dotted black line), and drag (dashed black line) *v.s.* $\overline{\mathbf{X}}$, b) nominal pitching moment input (dotted black line) and resulting pitching moment input (solid black line) *v.s.* $\overline{\mathbf{X}}$, c) nominal angle of attack (dotted black line) and resulting angle of attack (solid black line) *v.s.* $\overline{\mathbf{X}}$.

C. Filter transformation and reference injection gain

Given the closed loop state matrix: $A_{_F}=\overline{A}-FB=[a_{c_{ij}}]$, let us define the matrices:

$$
\overline{K}=\begin{bmatrix}
-a_{c_{21}} & -a_{c_{23}}-\frac{a_{c_{25}}\left(a_{c_{66}}^2+a_{c_{65}}\right)}{a_{c_{45}}}\\
-a_{c_{22}} & -a_{c_{24}}-\frac{a_{c_{26}}\left(a_{c_{66}}^2+a_{c_{65}}\right)}{a_{c_{45}}}\\
-a_{c_{45}}a_{c_{61}} & -a_{c_{45}}a_{c_{63}}\\
a_{c_{42}}a_{c_{65}}-a_{c_{45}}a_{c_{62}} & a_{c_{44}}a_{c_{65}}-a_{c_{45}}a_{c_{64}}\\
a_{c_{42}}a_{c_{66}} & a_{c_{44}}a_{c_{66}}-a_{c_{65}}\\
-a_{c_{42}} & -a_{c_{44}}-a_{c_{66}}
\end{bmatrix},
$$

$$
T=\begin{bmatrix}
0 & 1 & 0 & 0 & 0 & 0\\
1 & a_{c_{22}} & 0 & \frac{a_{c_{26}}}{a_{c_{45}}} & \frac{a_{c_{26}}a_{c_{66}}}{a_{c_{45}}} & T_{26}\\
0 & 0 & 0 & 0 & 0 & 1\\
0 & a_{c_{42}} & 0 & 0 & 1 & T_{46}\\
0 & 0 & 0 & \frac{1}{a_{c_{45}}} & \frac{a_{c_{66}}}{a_{c_{45}}} & T_{56}\\
0 & a_{c_{62}} & \frac{1}{a_{c_{45}}} & \frac{a_{c_{66}}}{a_{c_{45}}} & \frac{a_{c_{66}}^2+a_{c_{65}}}{a_{c_{45}}} & T_{66}
\end{bmatrix},
$$

where $T_{_{26}}=a_{c_{24}}+a_{c_{26}}(a_{c_{66}}^2+a_{c_{65}})/a_{c_{45}}$, $T_{46}=a_{c_{44}}+a_{c_{66}}$, $T_{56}=(a_{c_{66}}^2+a_{c_{65}})/a_{c_{45}}$, $T_{66}=a_{c_{64}}+(a_{c_{66}}(a_{c_{66}}^2+a_{c_{65}})+a_{c_{65}}a_{c_{66}})/a_{c_{45}}$.